First-principles study of luminescence in Ce-doped inorganic scintillators

A. Canning,[1,2] A. Chaudhry,[1,2] R. Boutchko,[1] and N. Grønbech-Jensen[1,2]
[1]*Lawrence Berkeley National Laboratory, 1 Cyclotron Road, Berkeley, California 94720, USA*
[2]*Department of Applied Science, University of California, Davis, California 95616, USA*
(Received 9 August 2010; published 23 March 2011)

Luminescence in Ce-doped materials corresponds to a transition from an excited state where the lowest Ce 5*d* level is filled [often called the $(Ce^{3+})^*$ state] to the ground state where a single 4*f* level is filled. We have performed theoretical calculations based on density functional theory to calculate the ground-state band structure of Ce-doped materials as well as the $(Ce^{3+})^*$ excited state. The excited-state calculations used a constrained occupancy approach by setting the occupation of the Ce 4*f* states to zero and allowing the first excited state above them to be filled. These calculations were performed on a set of Ce-doped materials that are known from experiment to be scintillators or nonscintillators to relate theoretically calculable parameters to measured scintillator performance. From these studies, we developed a set of criteria based on calculated parameters that are necessary characteristics for bright Ce-activated scintillators. Applying these criteria to about 100 new materials, we developed a list of candidate materials for new bright Ce-activated scintillators. After synthesis in powder form, one of these new materials (Ba_2YCl_7:Ce) was found to be a bright scintillator. This approach, involving first-principles calculations of modest computing requirements, was designed as a systematic, high-throughput method to aid in the discovery of new bright scintillator materials by prioritization and down-selection on the large number of potential new materials.

DOI: 10.1103/PhysRevB.83.125115 PACS number(s): 71.15.Qe, 71.20.Ps, 78.70.Ps

I. INTRODUCTION

Inorganic scintillators are extensively employed as radiation detector materials in many fields of applied and fundamental research, such as medical imaging, high-energy physics, oil exploration, astrophysics, and nuclear materials detection for homeland security, as well as other applications.[1,2] The ideal scintillator for γ-ray detection must have exceptional performance in terms of stopping power, luminosity, proportionality, speed, and cost. Recently, trivalent lanthanide dopants have received greater attention for fast and bright scintillators. In particular, Ce^{3+} is a favored dopant in many scintillators due to its allowed optical 5*d*-4*f* transition, which is relatively fast (∼20–40 ns), and it can be doped onto La,Y, Gd, and Lu sites of many high-density host materials. Consequently, some of the brightest known scintillators are Ce-doped, such as $LaBr_3$:Ce,[3] LuI_3:Ce,[4] and YI_3:Ce.[5] However, crystal growth and production costs remain challenging for these materials.[6,7]

First-principles calculations provide useful insight into chemical and electronic properties of materials, and hence can aid in the search for better materials or guide modification of existing materials.[8–11] The theoretical work presented in this paper is part of a larger project, "High-throughput Discovery of Improved Scintillation Materials," which aims to synthesize and characterize new materials in microcrystal form and select candidates for crystal growth.[12] The main aim of the theoretical studies presented here is to develop a fast method to select candidate Ce-activated scintillator materials for synthesis as well as complement the experimental work through simulations of promising synthesized materials. Preliminary results from our studies have been presented earlier.[13] In this paper, we give a detailed account of our first-principles calculations and extensive results obtained so far using more advanced calculations than presented in our previous work.

The basic mechanism for scintillation in a Ce-doped material is that an incident γ ray will produce a large number of electron-hole (*e*-*h*) pairs in the host material that transfer to the Ce site. The emission of light then corresponds to a 5*d*-4*f* transition on the Ce site from the Ce $[Xe]4f^0\ 5d^1$ excited state, usually referred to as $(Ce^{3+})^*$, to the Ce^{3+} ground state $[Xe]4f^1\ 5d^0$ (see Fig. 1). Trapping mechanisms on the host, such as self-trapped excitons, hole traps, or electron traps, can quench or reduce the transfer of energy to the Ce site (see, for example, Ref. 1 for a more detailed discussion of scintillator mechanisms and quenching processes).

Recently, there has been a growing interest in *ab initio* calculations of the properties of 5*d*-4*f* transitions of rare-earth ions in solids. Much of this resulted from the pioneering work of Dorenbos and collaborators, who in a series of papers compiled experimental data of this transition and derived semiempirical models for predicting properties of the 5*d*-4*f* transition and estimated the positioning of these states in the host gap.[14–17] Most of the *ab initio* calculations performed to date for rare-earth (RE^{3+}) doping use either cluster models based on Hartree-Fock or band-structure approaches based on density functional theory (DFT). Usually, in the embedded cluster calculations, to reduce computational costs, the dopant and the first-shell ions around the dopant are allowed to relax while the rest of the crystal is kept frozen in the crystalline geometry. This can give anomalous results,[18,19] and possible deficiencies of this local relaxation procedure were discussed recently by Gracia *et al.*[20] for Ce^{3+}-doped YAG ($Y_3Al_5O_{12}$). Cluster models also cannot give the positions of the conduction band (CB) and valence band (VB) of the host relative to the dopant states, which is closely related to luminescence properties.

In one of the earliest works using a DFT-based approach, Stephan *et al.*[21] studied 5*d*-4*f* transitions for a number of trivalent lanthanides using band-structure calculations. The

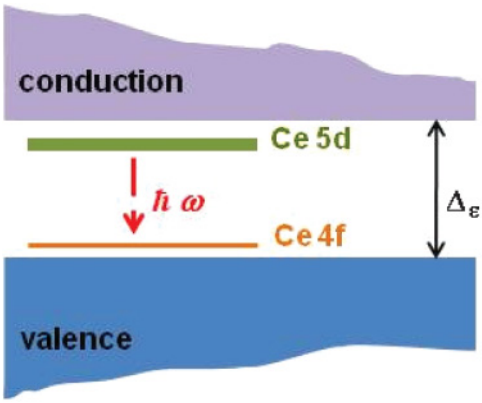

FIG. 1. (Color online) Schematic diagram for a Ce-activated scintillator showing the positions of the Ce 5*d* and 4*f* levels relative to the conduction and valence band of the host material. Δ_ε is the host material band gap.

effect of rare-earth (RE^{3+}) doping in semiconducting GaN has also been reported.[22] However, within the local-density approximation (LDA) or the generalized gradient approximation (GGA) to DFT, the self-interaction error associated with the localized nature of the 4*f* shell prohibits the calculation of accurate energy differences. There have been attempts to overcome this problem using methods that go beyond DFT, but they have focused on studies of bulk Ce compounds.[23,24] Recently, Nishida *et al.*[25] studied the relationship between the local structure around the Ce^{3+} ion and the emission properties of CeF_3 and Ce_2O_3 employing a combination of transmission electron microscopy–electron energy loss spectroscopy (TEM-EELS) measurements and first-principles band-structure studies. The 4*f*-5*d* energy gap was shown to be in qualitative agreement with known experimental spectra.

A band-structure approach can also be used to relax the doped host matrix to take into account lattice-relaxation effects. Andriessen *et al.*[26,27] have performed such relaxations for a few known Ce^{3+}-doped scintillating compounds. Recently, they have published detailed results for the Stokes shift from lattice-relaxation studies of 4*f*-5*d* excitation of Ce-doped lanthanum halide scintillators using a band-structure approach based on DFT and ionic cluster calculations using the Hartree-Fock method.[28] Watanabe *et al.*[29] studied the 4*f*-5*d* absorption spectra of Ce-doped $LiYF_4$ using a combination of the pseudopotential plane-wave method along with the relativistic molecular orbital approach. They found that the 4*f*-5*d* transitions in the case of Ce^{3+} can be attributed to transitions between molecular orbitals since Ce^{3+} has a simple $[Xe]4f^1$ electronic structure, implying that Ce 4*f*-5*d* transitions can be analyzed within the framework of a single-electron approximation.

Our theoretical calculations for the prediction of candidate scintillator materials are based on studies of the Ce 4*f* and 5*d* levels relative to the valence-band maximum (VBM) and conduction-band minimum (CBM) of the host material, respectively.[13] A necessary condition for scintillation and luminescence is that the Ce 4*f* and 5*d* levels must be in the gap of the host material. If the Ce 4*f* level lies in the valence band of the host or the 5*d* level is in the conduction band, there will be no Ce-activated scintillation or luminescence. If the 5*d* Ce state lies below but close to the bottom of the conduction band, then thermal excitation from the 5*d* state into the conduction band can reduce or quench luminescence. It should also be noted that under direct optical excitation of the 4*f*-5*d* transition, some Ce-doped systems can show strong luminescence but can be weak scintillators due to trapping mechanisms on the host that can quench or reduce the transfer of energy from the incident γ ray to the Ce site.

In the present paper, electronic-structure calculations of Ce-doped compounds are performed with the LDA+U (and GGA+U) approach.[30] This method has been shown in previous publications to give a better description of the localized 4*f* states of Ce compared to LDA or GGA.[24,31] We have tuned the empirical U_{eff} parameter for the Ce^{3+} impurity atom to match the calculated Ce 4*f* to host VBM gap with the experimental energy gap for some known scintillating and nonscintillating Ce-doped compounds. Validation and predictions of Ce 4*f*–VBM energy gaps in the ground state are presented.

An accurate determination of the Ce 5*d*–CBM energy gap for the $(Ce^{3+})^*$ state is difficult using standard ground-state LDA and GGA approximations to DFT. A ground-state calculation with the 4*f* level filled and the 5*d* level empty yields a 5*d* level that will be higher than when the 5*d* level is filled and the 4*f* level empty. The 4*f* level is closer to the nuclei than the 5*d* level, so when the 4*f* level is emptied, the screening effect from the positive nuclei will be reduced and the 5*d* level will move lower. The Stokes shift can also further lower the 5*d* level, but we did not try to model that in our simulations. Previous studies have found the Stokes shift to be difficult to model accurately with DFT-based band-structure codes.[28] We, therefore, performed excited-state (constrained LDA) calculations and subsequent analysis to allow us to derive a qualitative measure of the 5*d*–CBM energy gap. Our main aim is not an extremely accurate calculation of the 5*d* level position, but to determine whether it is below the CB as this determines if luminescence from the Ce site is possible. It should also be noted that the host dopant site in our studies is either La, Lu, Gd, or Y, so the CB has 5*d* or 4*d* character. Therefore, systematic errors due to the LDA-type treatment of the Ce 5*d* state will also be present in the determination of the CBM, yielding, particularly in the case of La, Lu, and Gd, a reasonably accurate 5*d*–CBM separation due to cancellation of errors. The size of the supercells in our calculations typically prohibited the use of more advanced many-body methods. Earlier studies of Ce-activated scintillators with the cluster-based Hartree-Fock method found that adding configuration interaction only had a minor influence on the results.[28] Overall, we want to develop a high throughput method for the screening of large numbers of new materials as candidates for bright Ce-activated scintillators, so we restrict our calculations to computationally fast first-principles methods that can yield good qualitative results.

II. CALCULATION DETAILS

To simulate a dopant in a periodic lattice, we use the supercell approach with periodic boundary conditions. We construct a large supercell from periodically repeating the unit cell of the host crystal and then replace one of the host

trivalent sites by a Ce atom. We then relax the atomic positions while keeping the cell dimensions fixed. Our basic aim in these studies is to model one Ce atom in an infinite host lattice; however, the supercell approach introduces spurious dopant-dopant interactions due to the periodic boundary conditions.[32] These interactions can cause a broadening of the impurity levels into bands and also modification of the valence- and conduction-band edges, which are the natural reference energies for the impurity states. We, therefore, perform size scaling studies to be sure the supercells we use are large enough to produce converged results for the properties of interest. Once we have relaxed the supercell, we perform a ground-state calculation to determine the position of the Ce 4*f* level relative to the VBM of the host material. The filled 4*f* level is typically very localized and atomic in nature and has almost no bandwidth, so the 4*f*–VBM gap is well defined.

To determine if the $(Ce^{3+})^*$ state lies below the CBM, we perform a constrained LDA (or GGA) calculation by setting the occupancy of the Ce 4*f* states to zero and filling the first state above the 4*f* levels. Previous calculations for the $(Ce^{3+})^*$ excited state have been performed by removing the Ce 4*f* states from the basis functions or creating a pseudopotential with Ce 4*f* states treated as core states.[26,28,33] Our method has the advantage that we can use the same basis set and pseudopotential for both excited-state and ground-state calculations allowing direct comparison of energies. We then look at the spatial distribution of this excited state to determine if it is localized on the Ce or is a delocalized CB character state. The level of localization of an electronic state does not have a strict mathematical definition, but for the purposes of our studies, we will define it as the percentage of the normalized electron density in a Voronoi cell centered on the Ce atom. We will also consider relative localization: a ratio of localization of a state on the cerium site to its next largest localization on a different cation (La, Lu, Gd, or Y). If the state has no localization (the percentage on the Ce atom is very low and the ratio is unity or below), then we can consider it is a host band-structure state and is the bottom of the CB. In such a scenario, any localized state of Ce 5*d* character lies above the CBM and there is no possibility of scintillation or luminescence. If the state is localized on the Ce and has 5*d* character, then we can associate it with the so-called $(Ce^{3+})^*$, and a 5*d*-4*f* transition is possible. We found this procedure for determining if there exists a $(Ce^{3+})^*$ state below the CBM necessary, as in the systems studied there typically seems to be some level of hybridization between the host *d* character CB and the Ce 5*d* character states. This will, to some degree, delocalize them from an atomiclike 5*d* state centered on the Ce. We, therefore, needed a simple way to characterize the lowest *d* type as a CB or Ce state without having to resort to very large supercell calculations where the electronic states and energies were completely converged. We found that for wave functions localized over many atomic distances, the percentage in the Voronoi cell as well as the ratio to neighboring cations can be low, even though to the eye the wave function is clearly localized in space. Our simple definition of localization does not contain any concept of localization distance and poorly characterizes states localized over many atomic distances. We will discuss this issue more in the Results section, where we find that some of the oxide scintillators such as YAP ($YAlO_3$:Ce) have $(Ce^{3+})^*$ states localized over many atomic distances. It should also be noted that very localized $(Ce^{3+})^*$ states will tend to have a larger binding energy due to Coulomb attraction between the 5*d* electron and the nuclei. The removal of the 4*f* electron reduces the screening of the positive nuclei or can be thought of as leaving a hole state (compared to the ground state), which has Coulomb attraction with the filled 5*d* state. The excited state will then have more of a chance of being lower in energy than native exciton states on the host, which might otherwise reduce or quench the scintillation. The Ce 5*d* character state lying below the CBM is a necessary, but not sufficient, condition for scintillation. Related to this, one of the goals of our work is to study how the Ce 5*d* state properties are related to scintillation as well as luminescence properties in Ce-doped materials.

A. Atomic relaxation studies

The initial atomic positions and symmetry information of the host crystal were taken from the Inorganic Crystal Structure Database (ICSD).[34,35] The number of atoms in the Ce-doped supercells was typically 50–150 depending on the size of the host unit cell and how many atoms were required for reasonable convergence. The Vienna *Ab initio* Simulation Package (VASP)[36–38] was used for spin-polarized GGA [Perdew-Burke-Ernzerhof (PBE)][39] and LDA calculations. The projector-augmented-wave-function (PAW) approach, developed by Blöchl[40] and adapted and implemented in VASP,[41] was used for the description of the electronic wave functions. Plane waves have been included up to an energy cutoff of 500 eV. Integration within the Brillouin zone was performed with a Γ-point centered grid of *k* points. The number of irreducible *k* points was typically chosen to be four or eight, depending on the size and geometry of the supercell. The energy convergence criterion was set to 10^{-6} eV and the maximum component of force acting on any atom for relaxation of the atomic positions after doping with cerium was checked to be less than 0.01 eV/Å in every direction. Cerium pseudopotential was chosen to include (5*s*,5*p*,6*s*,4*f*,5*d*) as valence electrons. We have used the rotationally invariant method of Dudarev[42] as implemented in VASP[43] for an on-site $+U$ correction to treat the cerium 4*f* electrons with a single-parameter $U_{\text{eff}} = U - J$, where the Hubbard U parameter is the spherically averaged screened Coulomb repulsion energy required for adding an extra electron to the Ce 4*f* states, and the parameter J adjusts the strength of the exchange interaction. We determined U_{eff} empirically by adjusting it to correspond to experimental results (see Sec. IV A). We did not use a $+U$ correction for the Ce 5*d* states because the standard LDA and GGA have been found to give reasonably good agreement with experiment for Ce 5*d* energy levels in the types of systems studied here.[28] An artifact of DFT-PBE (or LDA) calculations is that unoccupied La 4*f* states are positioned at the bottom of the conduction band.[11] However, La 4*f* states lie higher in energy,[44,45] so in our calculations we push the La 4*f* states higher in the energy plot using the LDA+U approach with the U_{eff} parameter taken from Ref. 46. Without this correction, LDA calculations can wrongly place the Ce 5*d* states above the La 4*f* states. Calculations for Gd systems were performed with the VASP Gd_3 (4*f* states in core) pseudopotential. We checked two test

calculations with the regular Gd pseudopotential (4*f* electrons as valence) and found the results to be very similar. We do not employ spin-orbit coupling in our calculations because in the case of the La halides this was found to only move the Ce 5*d* states by a maximum of about 0.2 eV,[28] which would not change our qualitative conclusions and would increase the computational cost.

For the purposes of comparison and checking the accuracy of the pseudopotentials, ground-state density-of-states (DOS) calculations were done for a few Ce-doped systems using the full-potential linear augmented-plane-wave (FP-LAPW) code WIEN2K.[47] The relaxed atomic positions from the VASP code were used as input to the WIEN2K code. The same GGA (PBE) functional was used in the two codes. We kept the *k*-point grid and energy convergence criteria similar to VASP calculations. The number of plane waves was restricted to $R_{\mathrm{MT}} \times k_{\mathrm{max}} = 7$. The fully localized limit (FLL) form of GGA+U implementation was used within the WIEN2K code to treat the Ce 4*f* orbital. The value of the U_{eff} parameter was kept the same in the two calculations. The results were found to be very similar to PAW calculations with VASP with the positions of the various bands varying by only a few percent between the two codes.

B. Excited-state calculations

To study the $(Ce^{3+})^*$ state, constrained LDA (and GGA) calculations were done at the Γ point using the VASP code. The occupation numbers were manually set to empty the Ce 4*f* states and fill the next highest state. The band decomposed charge density was subsequently analyzed to derive the localization parameters.

Excited-state calculations were also done within the PAW framework as implemented in the ABINIT code.[48–50] The electronic wave functions were expanded in plane waves up to a kinetic-energy cutoff of 60 Hartree. Self-consistency was achieved using a *k*-point grid centered at the Γ point in reciprocal space. The energy tolerance for the charge self-consistency convergence was set to 10^{-6} Hartree. Band-decomposed charge density at the lowest-energy *k* point was subsequently analyzed to derive the localization parameter. ABINIT calculations were, however, limited to compounds with elements having reliable PAW data sets.

III. THEORETICAL CRITERIA FOR SCINTILLATION AND LUMINESCENCE

Based on the present understanding of scintillation physics and our previous first-principles studies of known Ce^{3+} scintillators [e.g., $YAlO_3$:Ce (YAP), Lu_2SiO_5:Ce (LSO), $LaCl_3$:Ce, $LaBr_3$:Ce, LaI_3:Ce, $Lu_2Si_2O_7$:Ce (LPS), etc.] and non-Ce-activated scintillators [e.g., Y_2O_3:Ce, La_2O_3:Ce, $LaAlO_3$:Ce (LAP)], we have developed three criteria based on the following theoretically calculable parameters to predict candidate materials for bright Ce^{3+} activated scintillation.[13]

(i) The size of the host material band gap.

(ii) The energy difference between the VBM of the host and the Ce 4*f* level.

(iii) The level of localization of the lowest *d* character excited state needed to determine if it is a host CB state or a Ce 5*d* character state.

Criterion (i) is related to the fact that the number of electron-hole pairs produced by an incident γ ray is inversely proportional to the band-gap energy, although the constant of proportionality varies from material to material.[51] Therefore, the band gap should be as small as possible but must be large enough to accommodate the Ce 4*f* and 5*d* states. LDA and GGA are known to underestimate the band gap, but for the purposes of our calculations it does provide trends in families as well as comparative results for similar materials. More accurate band gaps can be calculated theoretically by using more advanced methods that go beyond LDA, but these methods are typically more computationally costly. Therefore, for the purposes of a qualitative prediction of candidate scintillator materials, we use LDA and GGA calculations of band gaps.

Criterion (ii) is related to the cases in which the energy transfer to the Ce site occurs by sequential hole trapping and electron trapping on the Ce site. For these cases, if the 4*f*–VBM gap is large there will be a low probability of the hole transferring from the host to the Ce site, which will reduce scintillation brightness. Also, if the 4*f* is in the VB there will be no scintillation.

Criterion (iii) as discussed in the previous section is how we determine if the lowest *d* character excited state can be associated with a Ce 5*d* character state or a conduction-band state of the host material depending on whether the state is localized or not.

A further expected result of our calculation may be an estimation of the Ce 5*d*–CBM gap. This is in fact extremely difficult to calculate accurately, as in our large supercells there are many *d* character bands associated with the host as well as those associated with Ce. The bands associated with Ce-localized 5*d* states, even with large supercells, typically still have some curvature due to finite-size effects, making the 5*d*–CBM gap not well defined. It is also a difficult process to scan up through the lowest *d* character bands to determine which are associated with Ce 5*d* states and which are CB character states, as most bands show some level of hybridization, particularly at higher energies and presumably close to the CBM. In many cases, the excited-state calculation is also slow or problematic to converge due to the close proximity of the many *d* character bands to the filled *d* band. This is also one of the reasons we have used different codes such as ABINIT and VASP for these calculations, as we have found that for different systems one code may have better convergence properties than the other due to the different minimization methods used. For some known scintillators and nonscintillators, we have performed more detailed studies of the character of the different *d* bands, and we will present this in future work. In particular, for some nonscintillators we do find 5*d* character Ce states within the conduction band, although they typically have some hybridization with the host *d* states. The problems in calculating a 5*d*–CBM gap are not shared in determining the 4*f*–VBM gap, as the 4*f* state is typically extremely localized on the Ce atom giving a flat band even with modest-sized supercells. The higher-energy empty 4*f* states are also well separated from the filled 4*f* states, giving fast convergence for the ground-state calculation.

From the point of view of predicting new bright scintillators, it would be useful to develop more theoretical criteria related to trapping processes on the host that can limit energy

transfer to the Ce site. Unfortunately, it is difficult to use first-principles calculations to develop criteria related to these host processes, as the exact nature of the trapping sites on the host is often poorly understood from experiment as well as the details of the energy-transfer mechanisms to the Ce site. For example, accurate calculations of deep self-trapped host excitons such as those found in LaF_3 often require advanced many-body theories and involve significant lattice relaxation. The dynamical nature of the transfer processes of host excitons and hole or electron traps to the Ce site is also difficult to model from first principles, although there has been work done in developing empirical models of these processes.[52] Overall though, from an energetics point of view, we would expect the transfer of energy to the Ce site to be most favored the deeper the $(Ce^{3+})^*$ state is within the band gap of the host material. For example, if the $(Ce^{3+})^*$ state is lower in energy than any host self-trapped excitons (STEs), it will preferentially form provided there are no large energy barriers to transfer processes from the host to the Ce site. As with semiconductor dopant states, the depth of the $(Ce^{3+})^*$ state in the gap of the host material will be related to its level of localization.[53] This is particularly true where the character of the CB and dopant state are the same, which is the case for the systems studied here. Hence we expect criterion (iii) to also be related to the brightness of a Ce-activated scintillator.

IV. RESULTS AND DISCUSSIONS

In this section, we present results of our theoretical studies on Ce-doped compounds. The discussion is divided into three subsections. The first subsection concerns the ground-state density of states calculations for Ce^{3+}-doped compounds, specifically the determination of the U_{eff} parameter from experimentally measured Ce 4*f*–VBM energy gaps. Cell size scaling studies were also performed to check the dependence of the U_{eff} parameter on the simulation supercell size. The second subsection presents results of the excited-state calculations. Simulation cell size scaling studies are also presented in this section. In the final subsection, we perform calculations for some new materials doped with Ce and apply our theoretical criteria for the prediction of new bright candidate Ce-activated scintillators. One of the new scintillators predicted by our calculations was synthesized in microcrystal form and confirmed to be relatively bright. We have also generated a database of Ce 4*f*–VBM energies predicted from first-principles calculations of more than 100 compounds.

A. Ground-state calculations: Determination of U_{eff} parameter

The U_{eff} is known to correct for the self-interaction energy error present in LDA and GGA calculations giving a more accurate description of very localized states such as the Ce 4*f* states. U_{eff} can be determined in a self-consistent way as demonstrated by Cococcioni *et al.*[54] for CeO_2. However, more frequently U_{eff} is chosen in such a way as to reproduce with reasonable accuracy an experimentally measured quantity like cell volume, bulk modulus, etc.[24,31,55] We are not aware of any prior publication related to LDA+*U*-type calculations for Ce-doped insulators of the type used for scintillator detectors.

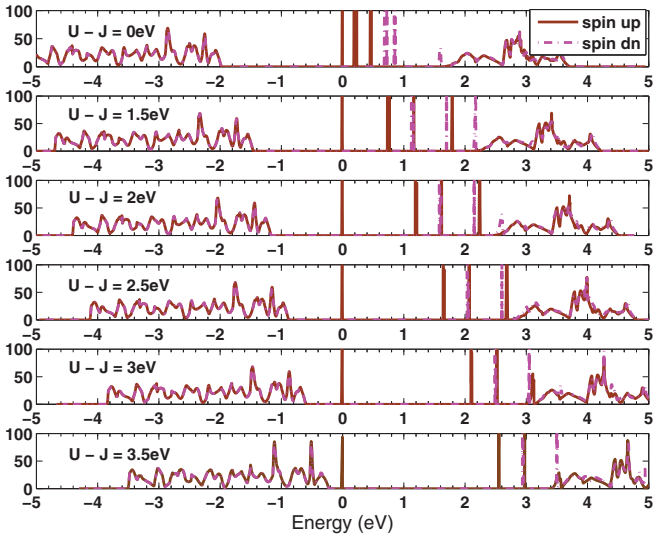

FIG. 2. (Color online) Ground-state DOS plot for $LaBr_3$:Ce from PBE+*U* spin-polarized calculations for different values of U_{eff}. Fermi level is set at 0. $U - J = 0$ eV corresponds to DFT-PBE result. Experimentally estimated 4*f*–VBM gap is 0.9 ± 0.4 eV.[56]

Fortunately, experimental measurements of the Ce 4*f*–VBM gap are known for a few scintillators, so we chose the U_{eff} parameter to closely match these known gaps.

Figure 2 shows the total density of states plot for $LaBr_3$:Ce for different values of the U_{eff} parameter from a GGA(PBE)+*U* calculation. The filled Ce 4*f* state is at the Fermi level, which is set to zero. The experimentally measured Ce 4*f*–VBM gap for $LaBr_3$:Ce is 0.9 eV (±0.4 eV).[56] We observe from the figure that the calculated 4*f*–VBM energy gap using $U_{\text{eff}} = 2.5$ eV matches the experimental data. It is important to note that the value of U_{eff} used in the literature for bulk Ce(III) compounds ($U_{\text{eff}} = 4.5$ eV for the PBE functional[24,57]) is different from our results. This is mainly due to the itinerant nature of 4*f* electrons in Ce bulk compounds, which participate in bonding compared to our doped ionic systems where the single Ce 4*f* electron is atomiclike in nature. Hence it is important to tune the empirical parameter U_{eff} to get a close match with experimental data for Ce-doped scintillator materials. It should also be noted in these DOS plots that the filled Ce 4*f* state is close to being a δ function corresponding to a flat band. The 4*f*–VBM gap is therefore well defined from band-structure calculations for these types of system.

Figure 3 shows total DOS plots of $Lu_2Si_2O_7$:Ce (LPS) for different simulation cell sizes for a fixed U_{eff} parameter. Even for these small cell sizes, there is negligible variation in the Ce 4*f*–VBM energy gap (∼2%) with cell size. All the data presented in Table I are for similar or larger cell sizes, so we are confident that any finite-size effects on the Ce 4*f*–VBM energy gap are below a few percent. However, as we show in the next subsection, simulation cell size has a greater influence on the localization of the excited state.

We repeated the calculations for a few systems such as YI_3:Ce and $LaBr_3$:Ce using the LDA+*U* functional, and we found negligible change in the results compared to GGA(PBE)+*U* calculations. The choice of the approximation

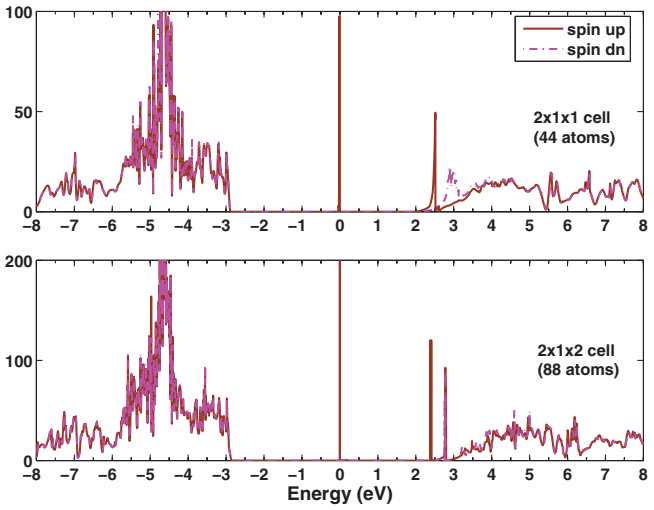

FIG. 3. (Color online) DOS plot for $Lu_2Si_2O_7$:Ce from PBE+U ($U - J = 2.5$ eV) spin-polarized calculations for two different cell sizes.

to the exchange-correlation functional (PBE or LDA) does not affect the position of the impurity (Ce) 4*f* levels. This is unlike calculations for bulk Ce compounds where different values of U_{eff} have been used for different functionals.[57] This is because the Ce 4*f* atomiclike character changes little for the different functionals.

Table I summarizes the results of our studies to tune the Ce 4*f*–VBM to known experimental measurements for Ce-doped materials. We see from Table I that GGA(PBE)+U calculations with a $U_{\text{eff}} = 2.5$ eV give good agreement with experimentally measured Ce 4*f*–VBM gaps for most materials with the exception of LaI_3:Ce, where $U_{\text{eff}} = 2.2$ eV gave the best agreement with experiment. LaI_3:Ce is one of the smallest band-gap scintillator materials, so the bonding is more covalent in nature than in other scintillator materials. This may account for the slightly different character of the Ce 4*f* state requiring a 0.3 eV lower value of U_{eff} than in the other systems. For many of the experimental results reported in the table, error bars are not quoted in the publications. We have found that in scintillator materials, the character of the Ce 4*f* is extremely atomic and very similar for different hosts, which explains the universality of the U_{eff} value in this class of materials. In the case of the heavier host La halides, there may be some weak dependence of the character of the Ce 4*f* on the local environment surrounding it. Oxides typically have a larger 4*f*–VBM gap than the heavier halides. The U_{eff} parameter we found that gives the best fit to experiment has no variation from oxides to halides and thus provides a potentially simple method to find the Ce 4*f*–VBM gaps for different types of compounds as compared to precise measurements.[65] In our calculations reported in subsequent sections for new materials, we used $U_{\text{eff}} = 2.5$ eV to correct the 4*f* position except for iodides and sulfides, where we used 2.2 eV.

TABLE I. Experimentally measured and calculated (PBE+U) 4*f*–VBM gaps for known Ce-activated scintillators and nonscintillators.

Compound	Measured 4*f*–VBM gap (eV)	PBE+U result (eV)
$LaBr_3$:Ce	0.9 ± 0.4	0.9
(scintillator)	(Dorenbos *et al.*[56])	($U_{\text{eff}} = 2.5$ eV)
$Lu_2Si_2O_7$:Ce	2.9	2.9
(scintillator)	(Pidol *et al.*[58])	($U_{\text{eff}} = 2.5$ eV)
Lu_2SiO_5:Ce	3.1	2.7, 2.9
(scintillator)	(Joubert *et al.*[59])	($U_{\text{eff}} = 2.5$ eV) two substitution sites
$YAlO_3$:Ce	~3.3	3.0
(scintillator)	(Nikl *et al.*[60])	($U_{\text{eff}} = 2.5$ eV)
LaI_3:Ce	0.2–0.3	0.25
(weak scintillator)	(Bessiere *et al.*[61])	($U_{\text{eff}} = 2.2$ eV)
YPO_4:Ce	~4.0	3.65
(weak scintillator)	(Dorenbos [62])	($U_{\text{eff}} = 2.5$ eV)
$LaAlO_3$:Ce	~2.0	2.1
(nonscintillator)	(van der Kolk *et al.*[63])	($U_{\text{eff}} = 2.5$ eV)
La_2O_3:Ce	~2.8	2.9
(nonscintillator)	(Yen *et al.*[64])	($U_{\text{eff}} = 2.5$ eV)
Y_2O_3:Ce	~3.4	3.4
(nonscintillator)	(Pedrini *et al.*[65])	($U_{\text{eff}} = 2.5$ eV)

In all the systems studied, we found the 4*f* level to be above the VBM, so unlike the 5*d* level relative to the CBM, the 4*f* level position relative to the VBM is not a factor in preventing 5*d*-4*f* emission in Ce-doped systems

Our studies also revealed that ionic relaxation was predominantly influenced by the difference between Ce^{3+} ionic radii and the trivalent host cation dopant site with the choice of U_{eff} parameter having a negligible effect. Ce-doped Lu^{3+} and Y^{3+} compounds showed significant relaxation as compared to La^{3+} compounds primarily because of the almost 10% size mismatch between Ce^{3+} and Lu^{3+}, Y^{3+}, and less than 1% mismatch between the ionic radii of Ce^{3+} and La^{3+}.

B. Excited-state calculations

As described in Sec. II B, we performed excited-state calculations by manually setting the occupation of all the Ce 4*f* states to zero and filling the next highest state. Figures 4(a) and 4(b) shows the atom projected partial density of states for $Lu_2Si_2O_7$:Ce (LPS) in the ground state and excited state. There is no atomic relaxation in the excited state, so there is no Stokes shift in our calculations. For this system, the valence band of the host material consists of O *p* states hybridized with Lu 4*f* states, and the conduction band consists of Lu 5*d* character states. We can see from the ground-state plot that there are Ce 5*d* states below the Lu 5*d* states even in the ground-states DOS, and these move about 0.5 eV lower relative to the CBM in the excited-state plot. In the excited state plot, the excited-Fermi level lies above the lowest Ce 5*d* level showing the filling of the lowest Ce 5*d* level. In this system, the lowest Ce 5*d* levels are clearly below the host CB, as is necessary for the Ce 5*d*-4*f* transition to occur. As can be seen from this plot, the Ce 5*d* levels have some bandwidth resulting in a continuous DOS function for the Ce 5*d* states rather than the δ-type function we find for the very localized Ce 4*f* states. The higher-energy Ce 5*d* character states are hybridized with the Lu 5*d* states.

Figure 5 shows the atom projected partial density of states for Ce-doped $LaBr_3$ in the ground state, which, unlike LPS, is more typical of the type of result we obtained for different

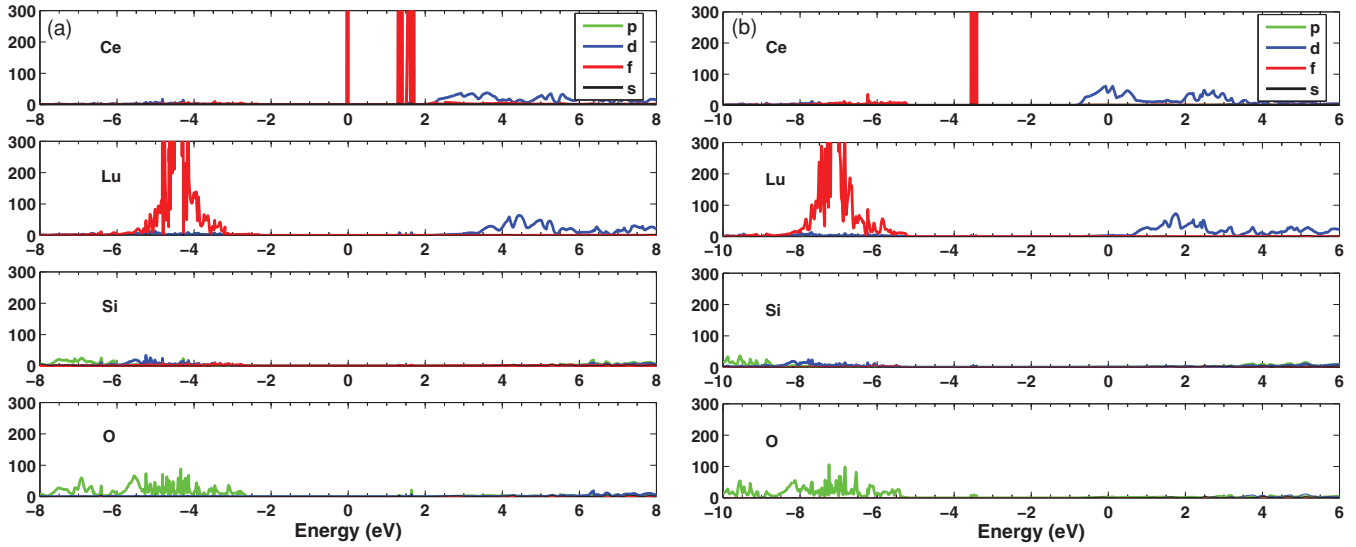

FIG. 4. (Color) Atom-projected partial DOS plots for GGA (PBE) calculations of Ce-doped $Lu_2Si_2O_7$ in the ground state (a) and excited state (b). Fermi level is set to 0. *f* character states are shown in red, *d* states in blue, *p* characters states in green, and *s* character states are shown in black.

scintillators. The 5*d* states on the La and Ce are hybridized and occur at the same energy, so there are no well-defined Ce character 5*d* states below the CB. For these types of systems, we find the characterization of the lowest filled excited *d* state in terms of its localization on Ce to be the best method to determine if it has Ce 5*d* character or is a host CB character state.

Figure 6 shows charge-density isosurface plots of the first *d* character excited state at the Γ point for some known scintillators and nonscintillators. For the known nonscintillators La_2O_3:Ce, Y_2O_3:Ce, and $LaAlO_3$:Ce, there is no localization on the Ce and the excited state has a band-structure character distributed throughout the supercell. On the other hand, a localized excited state with *d* character forms on the Ce site for the known scintillators $Lu_2Si_2O_7$:Ce, $LaBr_3$:Ce,

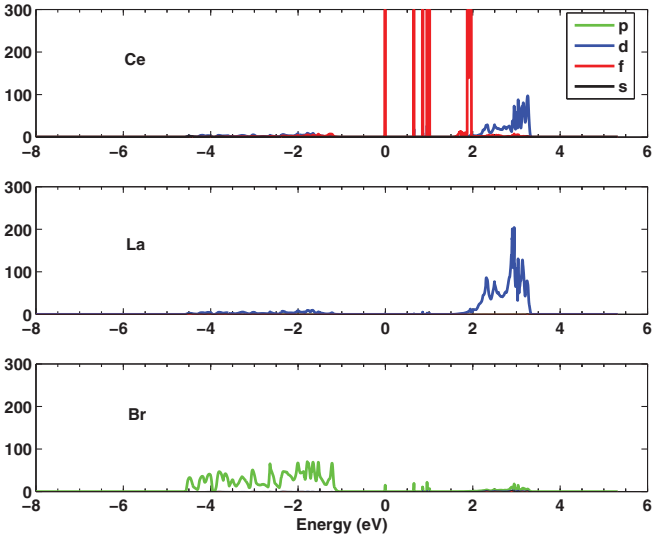

FIG. 5. (Color) Atom-projected partial density of states plots for $LaBr_3$:Ce in the ground state. Fermi level is set at 0 eV. Calculation used the (GGA) PBE functional and ABINIT code.

and $YAlO_3$:Ce. As can be seen from the plots, there is a large range of localization of the excited state, with $Lu_2Si_2O_7$:Ce being much more localized than the other systems.

Table II presents a list of our theoretically calculated parameters of band gap, 4*f*–VBM gap, % localization, and localization ratio for a list of known scintillators and nonscintillators compared to experimental data for band gaps and scintillation luminosity. As expected, LDA consistently underestimates the band gap but does correctly predict the ordering of band gaps for similar materials and families of materials. In all these materials, the Ce 4*f* level is above the VBM, so the occurrence of the 4*f* level within the VB never seems to be a factor in quenching luminescence and scintillation in Ce-doped materials. Also, to the best of our knowledge, there is no experimental evidence of Ce 4*f* states inside the host VB. The main result from this table is that we have essentially no localization of the lowest excited *d* state for all the nonscintillators. The brightest scintillators typically have low band gaps and small 4*f*–VBM gaps, although it should be noted that for scintillation the band gap has to be large enough to accommodate the Ce 4*f* and 5*d* states. Overall, there is good qualitative agreement between our three criteria and bright scintillators.

The La halides represent a family of materials that have been very heavily studied experimentally for Ce activation, as they are all scintillators and have a large range of band gaps. LaI_3:Ce has a very low band gap of 3.3 eV and is thermally quenched at room temperature due to the proximity of the excited Ce state to the CBM, but it has reasonable luminosity at 100 K.[61] Excited-state calculations for this system are particularly difficult to converge since Ce 5*d* states hybridize and are very close to the host CB. This is consistent with the experimentally estimated 5*d*–CBM gap of ∼0.2 eV.[61] This also leads to relatively low values for the % localization and ratio. The $(Ce^{3+})^*$ excited state is favorably localized for $LaCl_3$:Ce and $LaBr_3$:Ce. This agrees with the fact that these materials are well-known bright scintillators used in several

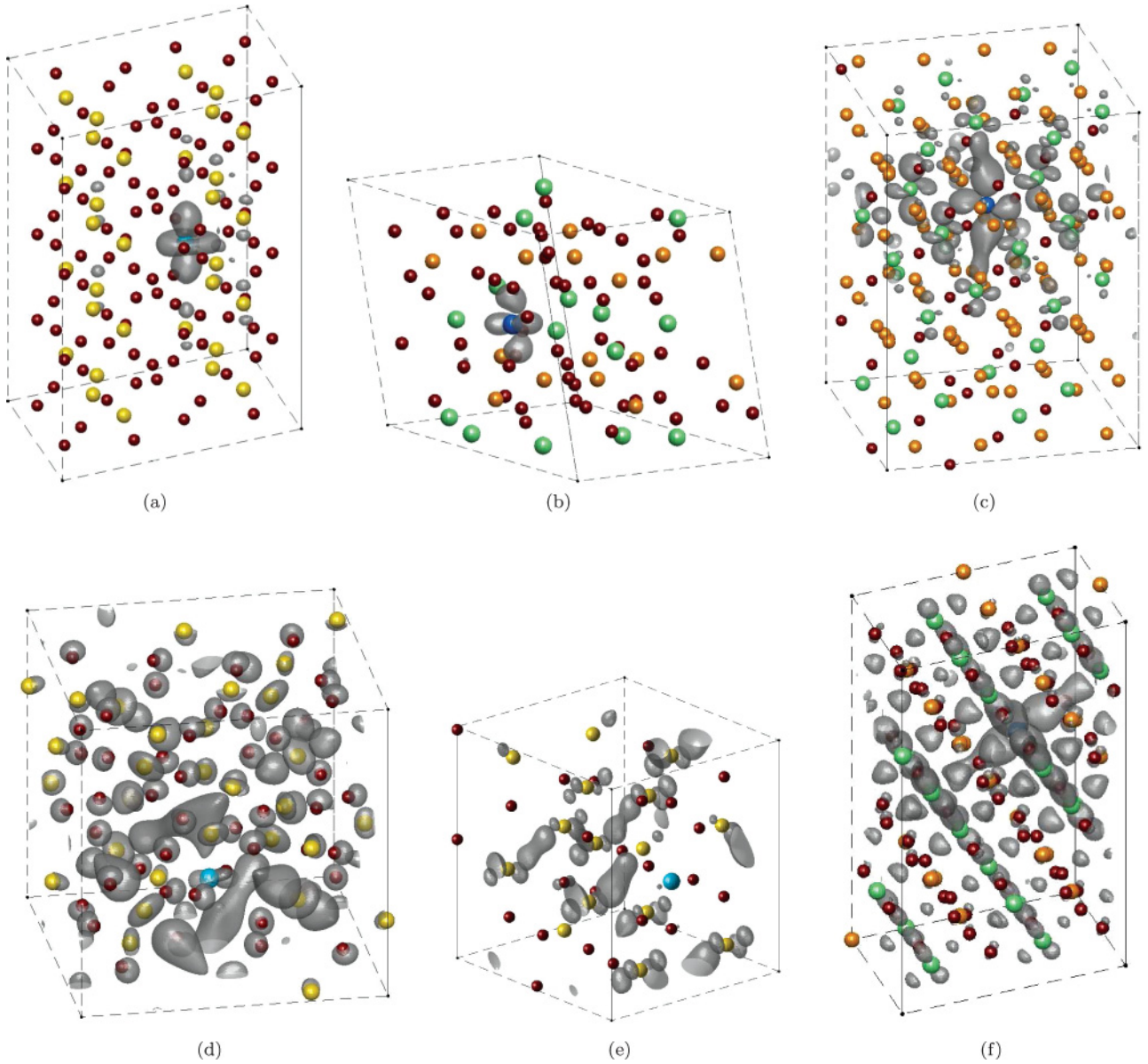

FIG. 6. (Color) Lowest *d* character excited-state plots for Ce scintillators and nonscintillators. Plots show charge-density isosurfaces of the excited states. Ce atom is shown in blue, rare-earth ion (= La, Lu, Y) is in yellow, and the anions are shown in red. (a) $LaBr_3$; (b) $Lu_2Si_2O_7$; (c) $YAlO_3$; (d) Y_2O_3; (e) La_2O_3; (f) $LaAlO_3$. The excited state is delocalized (very little or no concentration around Ce site) for nonscintillating compounds La_2O_3:Ce, Y_2O_3:Ce, and $LaAlO_3$:Ce. However, Ce^{3+} scintillators have good localization of the excited state on the Ce site.

γ-ray detection applications.[2] $LaBr_3$:Ce in particular has a lower band gap, a favorable 4*f*–VBM gap, and reasonable localization on the Ce site. It should be noted that the role of host STEs is known to be important in the transfer of energy to the Ce site for $LaCl_3$:Ce and $LaBr_3$:Ce, where the transfer mechanism is efficient, leading to bright scintillators. In these cases, the size of the 4*f*–VBM gap will play less of a role in determining the brightness.[52] LaF_3:Ce is an example of a system that is known to have a very deep STE of a lower energy than the $(Ce^{3+})^*$ excited state.[66] Even though the lowest *d* character excited state is of Ce 5*d* character and well localized, this limits the transfer of energy to the Ce site and results in very low luminosity for this particular material. Moreover, the band gap and 4*f*–VBM energy gap for this system are quite large, which leads to comparatively lower *e*-*h* pair production and a low probability of sequential hole and electron capture by Ce. Thus, even if there were no low-energy host STEs, we would not expect this system to be a bright scintillator.

Oxide scintillators in general have wider band gaps than heavy halide scintillators, so Ce 4*f* and 5*d* states are mostly better separated from the band edges. As we can see from Table II, the $(Ce^{3+})^*$ state is favorably localized in most of these systems. $YAlO_3$:Ce is an example of a system that has a rather low % localization and ratio, even though Fig. 6 clearly shows a localized state. The main reason for this is that the state is localized over a few interatomic spacings, so since our simple measures of localization have no measure of

TABLE II. Calculated DFT-PBE band gaps and energy differences for known Ce-activated scintillators and nonscintillators. Experimental luminosity data in photons/MeV are taken from Ref. 67 and the references therein. Asterisks corresponds to no observed Ce emission.

Compound	PBE band gap[a]	Ce 4*f*–VBM gap	$(Ce^{3+})^*$ Localization		Luminosity
(atoms in supercell)	(eV)	(eV)	%	Ratio	(photons/MeV)
LaF_3 (48)	7.8 (9.7) (Ref. 68)	3.5	46	9.14	2200
$LaCl_3$ (128)	4.6 (7) (Ref. 69)	1.4	40	6.08	48000
$LaBr_3$ (128)	3.6 (5.9) (Ref. 56)	0.9	21	5.70	74000
LaI_3 (64)	1.6 (3.3) (Ref. 61)	0.25	18	2.52	200–300[b]
$LaMgB_5O_{10}$ (68)	5.7 (8.8)(Ref. 79)	2.6	18	2.48	1300
YI_3 (384)	2.8 ($\sim$ 4.13) (Ref. 70)	0.6	31	3.48	98600
$YAlO_3$ (160)	5.4 (8.5–8.9) (Refs. 71 and 72)	3.0	21	3.17	21600
$LiGdCl_4$ (96)	4.6	1.4	74	27.6	64600
$Lu_2Si_2O_7$ (88)	5.5 (7.8) (Ref. 58)	2.9	55	6.8	26000
Lu_2SiO_5 (64)	4.8 (6.6) (Ref. 59)	2.9	33	7.3	33000
Cs_2LiYCl_6 (40)	5.0 ($>$ 5.9) (Ref. 73)	1.8	50	5.8	21600
β-KYP_2O_7 (88)	5.9 ($\sim$7.7) (Ref. 74)	2.7	35	6.4	10000
$LaAlO_3$ (120)	4.0 (5.5) (Ref. 63)	2.1	4	1.6	**
Y_2O_3 (80)	4.6 (5.8) (Ref. 75)	3.4	2	0.63	**
La_2O_3 (40)	4.0 (5.3–5.8) (Ref. 64)	2.9	1	0.15	**
Lu_2O_3 (80)	4.7 (5.8)(Ref. 80)	2.9	2	1.1	**
Gd_2O_3 (80)	4.4 (5.4)(Ref. 81)	2.8	4	0.9	**

[a]The value in parentheses refers to known experimental band gaps.
[b]Luminosity 16 000 ph/MeV at 100 K.

localization with distance from the Ce, they tend to give low values for these types of localized states.

We also studied the dependence of localization of the excited state with cell size. As an example, Fig. 7 shows the localization of a bright scintillator YI_3:Ce with increasing cell size. YI_3 has a trigonal crystal structure with $a = b =$ 7.4864 Å and $c = 20.88$ Å. In the excited-state plot for the 24-atom conventional unit cell, even though the dopant Ce^{3+} ion has a high percentage localization, the ratio to the next highest Y^{3+} indicates that Ce sites in the periodically repeated cells are interacting with each other in the direction of the shortest cell dimension (horizontal plane containing the Ce atom and the neighboring Y). Now when we scale in the horizontal dimensions for the 96-atom simulation cell, we find that the Y atoms in the same plane as Ce have some fraction of the excited state, but Ce has the highest percentage of the localization of the excited state. This, still, does not clearly show a predominating Ce localization expected of a bright scintillator like YI_3:Ce because the excited-state wave function is not well localized within the cell volume and, consequently, there is interaction with the Ce sites in the periodically repeated cells in the plane containing lattice vectors a and b. Upon scaling the simulation cell size to 384 atoms, the excited state becomes predominantly concentrated on the Ce site. We found that the convergence with cell size varied significantly for different host materials. The cell sizes quoted in Table II were chosen to give well-converged results for the materials studied, and are typically smaller than for YI_3:Ce.

C. Prediction of new candidate Ce scintillators

The next step in our studies was to look at new candidate scintillators. The criteria we developed from studying known scintillators and nonscintillators were applied to the prediction of new candidate scintillators. We chose new host compounds based on their γ-ray stopping power and suitability for doping with Ce (i.e., hosts with trivalent sites such as Y, La, Lu, or Gd for substitution by a Ce atom). We have performed calculations

TABLE III. Calculated band gaps, 4*f*–VBM separation, and localization for new Ce-doped compounds.

Compound	LDA band gap	Ce 4*f*–VBM gap	$(Ce^{3+})^*$ Localization	
(atoms in supercell)	(eV)	(eV)	%	Ratio
$CsLa(SO_4)_2$ (48)	6.0	2.0	44	7.5
Ba_2YCl_7 (40)	4.7	1.6	71.7	13.2
GdIS (96)	2.5	1.3	17	1.9
$BaY_6Si_3B_6O_{24}F_2$ (46)	4.6	1.3	78	15.2
Gd_2SCl_4 (112)	3.6	1.0	31.5	2.04
$Cs_3Y_2Br_9$ (84)	3.0	1.2	34	2.69

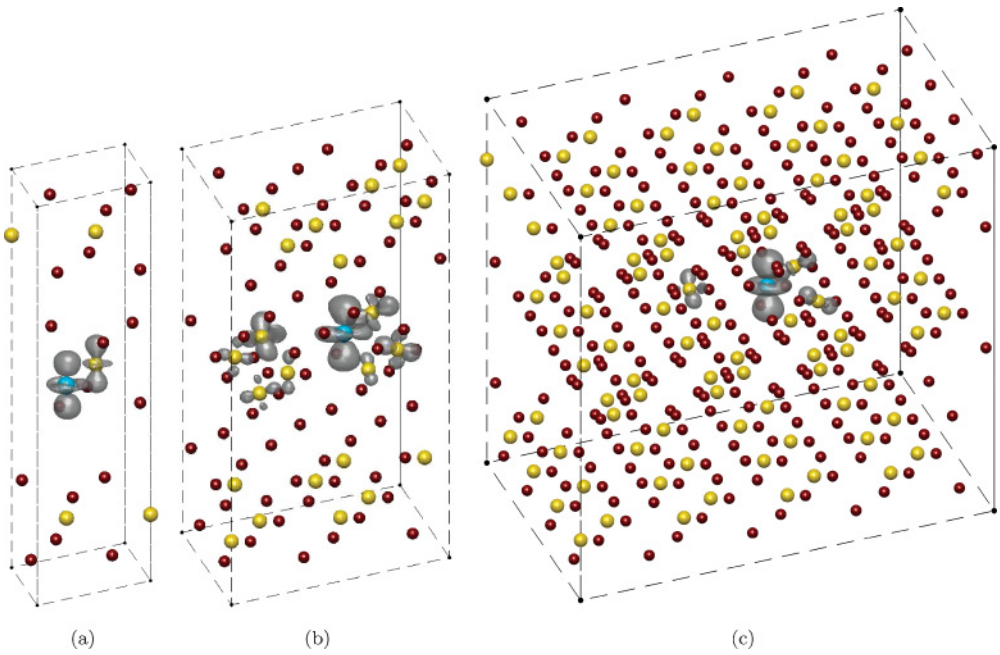

FIG. 7. (Color) Excited-state charge-density isosurface plots of YI_3:Ce showing the effect of scaling the simulation cell size. All plots are shown at the same isosurface threshold. Ce atom is shown in blue, Y is in yellow, and iodine atoms are shown in red. (a) $1 \times 1 \times 1$ cell (24 atoms); (b) $2 \times 2 \times 1$ cell (96 atoms); (c) $4 \times 4 \times 1$ cell (384 atoms). $(Ce^{3+})^*$ excited-state localization numbers for these plots are (a) (40%, 1.61); (b) (21%, 2.67); and (c) (31.1%, 3.48).

for about 100 new host compounds. The new materials we have studied with the best characteristics for bright Ce activation are listed in Table III.

In particular, the $(Ce^{3+})^*$ state for Ba_2YCl_7:Ce was found to have one of the highest levels of localization of all the systems studied (see Fig. 8). The band gap and 4*f*–VBM separation have values that are close to those of some of the well-known bright scintillators. Therefore, on the basis of our theoretical criteria outlined in Sec. III, Ba_2YCl_7:Ce was expected to be a good candidate for a bright new scintillator. It was subsequently synthesized and found to be bright in microcrystal form.[76] In terms of predictions of nonscintillators, we have studied many other families of materials and have found that for all Y and La host materials containing Ti, Zr, and Hf, there is no localized excited Ce state below the conduction band. Ce^{3+} doping in Bi^{3+} host compounds also leads to no localized Ce 5*d* state below the conduction band. Some of these studies will be the subject of future publications. We have also previously published theoretical work on Ce-doped Y and La oxyhalides[77] as well as Y halides,[78] which included known as well as new scintillators.

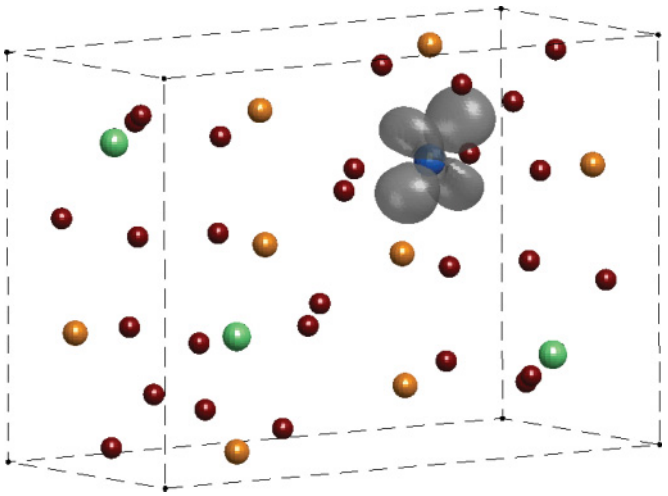

FIG. 8. (Color) $(Ce^{3+})^*$ excited-state plot for Ba_2YCl_7:Ce at 50% isosurface threshold. Ce is shown in blue, Ba in orange, Y is in green, and the Cl ions are shown in red.

V. CONCLUSIONS

In this paper, we have presented DFT-based first-principles studies for Ce-activated scintillator detectors. The main aim of this work was to determine what theoretically calculable parameters are easily related to luminescence and scintillation. To more accurately calculate the 4*f*–VBM position, we used the LDA+U approach, where we determined U_{eff} by comparison with experimental results. We found that a value of U_{eff} of 2.5 eV gave good agreement with experiment for a wide range of scintillator materials. Based on this, we have calculated the 4*f*–VBM gap for many known and new materials, some of which are presented in Tables II and III. We have also generated a database of Ce $4f$–VBM energies predicted from first-principles calculations for more than 100 new compounds. We also performed excited-state calculations using a constrained LDA approach to determine if the first excited *d* character state was localized on the Ce or was of conduction-band character. From these studies, we developed a set of theoretically calculable criteria that characterize bright Ce scintillation. We then validated these criteria by studying known scintillators and nonscintillators. These criteria were

then calculated for about 100 new materials to determine if they were candidates for bright Ce activation. The best candidates are listed in Table III. This approach, involving first-principles calculations of modest computing requirements, was designed as a systematic, high-throughput method to aid in the discovery of new bright Ce-activated scintillator materials. This approach has also been extended to Eu- and Pr-doped systems, which will be reported in future publications.

ACKNOWLEDGMENTS

We would like to thank Stephen Derenzo, Marvin J. Weber, Edith Bourret-Courchesne, and Gregory Bizarri for many invaluable discussions and constructive criticism. The work presented in this paper was supported by the US Department of Homeland Security and was carried out at the Lawrence Berkeley National Laboratory under US Department of Energy Contract No. DE-AC02-05CH11231.

[1] P. A. Rodnyi, *Physical Processes in Inorganic Scintillators* (CRC, Boca Raton, FL, 1997).
[2] C. W. E. van Eijk, Radiat. Prot. Dosim. **129**, 13 (2008).
[3] E. van Loef, P. Dorenbos, C. van Eijk, K. Kramer, and H. Gudel, Appl. Phys. Lett. **79**, 1573 (2001).
[4] K. Shah, J. Glodo, M. Klugerman, W. Higgins, T. Gupta, P. Wong, W. Moses, S. Derenzo, M. Weber, and P. Dorenbos, IEEE Trans. Nucl. Sci. **51**, 2302 (2004).
[5] J. Glodo, E. van Loef, W. Higgins, K. Shah, R. Devices, and M. Watertown, IEEE Trans. Nucl. Sci. **55**, 1496 (2008).
[6] E. V. van Loef, W. M. Higgins, J. Glodo, A. Churilov, and K. S. Shah, J. Cryst. Growth **310**, 2090 (2008).
[7] A. Iltis, M. Mayhugh, P. Menge, C. Rozsa, O. Selles, and V. Solovyev, Nucl. Instrum. Methods Phys. Res. A **563**, 359 (2006).
[8] S. Derenzo and M. Weber, Nucl. Instrum. Methods Phys. Res. A **422**, 111 (1999).
[9] M. Klintenberg, S. Derenzo, and M. Weber, Nucl. Instrum. Methods Phys. Res. A **486**, 298 (2002).
[10] V. Lordi, D. Åberg, P. Erhart, and K. J. Wu, Proc. SPIE, **6706**, 67060O (2007).
[11] D. Singh, H. Takenaka, G. Jellison Jr., and L. Boatner, in *Materials Research Society Symposia Proceedings Vol. 1038, Warrendale, PA* (MRS, Pittsburgh, 2008), p. 1038O0201.
[12] S. Derenzo *et al.*, IEEE Trans. Nucl. Sci. **55**, 1458 (2008).
[13] A. Canning, R. Boutchko, A. Chaudhry, and S. Derenzo, IEEE Trans. Nucl. Sci. **56**, 944 (2009).
[14] P. Dorenbos, J. Lumin. **91**, 91 (2000).
[15] P. Dorenbos, J. Lumin. **91**, 155 (2000).
[16] P. Dorenbos, Phys. Rev. B **62**, 15650 (2000).
[17] P. Dorenbos, Phys. Rev. B **64**, 125117 (2001).
[18] Z. Barandiarán, N. Edelstein, B. Ordejón, F. Ruipérez, and L. Seijo, J. Solid State Chem. **178**, 464 (2005).
[19] J. L. Pascual, J. Schamps, Z. Barandiaran, and L. Seijo, Phys. Rev. B **74**, 104105 (2006).
[20] J. Gracia, L. Seijo, Z. Barandiaran, D. Curulla, H. Niemansverdriet, and W. van Gennip, J. Lumin. **128**, 1248 (2008).
[21] M. Stephan, M. Zachau, M. Groting, O. Karplak, V. Eyert, K. Mishra, and P. Schmidt, J. Lumin. **114**, 255 (2005).
[22] K. C. Mishra, V. Eyert, and P. C. Schmidt, Z. Phys. Chem. **221**, 1663 (2007).
[23] L. Petit, A. Svane, Z. Szotek, and W. M. Temmerman, Phys. Rev. B **72**, 205118 (2005).
[24] C. Loschen, J. Carrasco, K. M. Neyman, and F. Illas, Phys. Rev. B **75**, 035115 (2007).
[25] I. Nishida, K. Tatsumi, and S. Muto, Mater. Trans. **50**, 952 (2009).
[26] M. Marsman, J. Andriessen, and C. W. E. van Eijk, Phys. Rev. B **61**, 16477 (2000).
[27] J. Andriessen, P. Dorenbos, and C. W. E. van Eijk, Phys. Rev. B **72**, 045129 (2005).
[28] J. Andriessen, E. van der Kolk, and P. Dorenbos, Phys. Rev. B **76**, 075124 (2007).
[29] S. Watanabe and K. Ogasawara, J. Phys. Soc. Jpn. **77**, 084702 (2008).
[30] V. Anisimov, F. Aryasetiawan, and A. Lichtenstein, J. Phys. Condens. Matter **9**, 767 (1997).
[31] D. A. Andersson, S. I. Simak, B. Johansson, I. A. Abrikosov, and N. V. Skorodumova, Phys. Rev. B **75**, 035109 (2007).
[32] R. M. Nieminen, Top. Appl. Phys. **104**, 29 (2007).
[33] M. Klintenberg, M. Weber, C. Dujardin, O. Eriksson, and S. Derenzo, Radiat. Eff. Defects Solids **154**, 231 (2001).
[34] G. Bergerhoff, R. Hundt, R. Sievers, and I. D. Brown, J. Chem. Inf. Comp. Sci. **23**, 66 (1983).
[35] ICSD (Inorganic Crystal Structure Database) (2009), [http://www.fiz-karlsruhe.de/icsd.html].
[36] G. Kresse and J. Hafner, Phys. Rev. B **47**, 558 (1993).
[37] G. Kresse and J. Furthmuller, Phys. Rev. B **54**, 11169 (1996).
[38] G. Kresse and J. Furthmuller, Comput. Mater. Sci. **6**, 15 (1996).
[39] J. P. Perdew, K. Burke, and M. Ernzerhof, Phys. Rev. Lett. **77**, 3865 (1996).
[40] P. E. Blöchl, Phys. Rev. B **50**, 17953 (1994).
[41] G. Kresse and D. Joubert, Phys. Rev. B **59**, 1758 (1999).
[42] S. L. Dudarev, G. A. Botton, S. Y. Savrasov, C. J. Humphreys, and A. P. Sutton, Phys. Rev. B **57**, 1505 (1998).
[43] A. Rohrbach, J. Hafner, and G. Kresse, J. Phys. Condens. Matter **15**, 979 (2003).
[44] J. Lang, Y. Baer, and P. Cox, J. Phys. F **11**, 121 (1981).
[45] M. T. Czyżyk and G. A. Sawatzky, Phys. Rev. B **49**, 14211 (1994).
[46] S. Okamoto, A. J. Millis, and N. A. Spaldin, Phys. Rev. Lett. **97**, 056802 (2006).
[47] P. Blaha, K. Schwarz, G. K. H. Madsen, D. Kvasnicka, and J. Luitz, *Wien2k, An Augmented-Plane-wave + Local Orbitals Program for Calculating Crystal Properties* (Technical Universität Wien, Austria, 2001).
[48] X. Gonze *et al.*, Z. Kristallogr. **220**, 558 (2005).
[49] X. Gonze *et al.*, Comput. Phys. Commun. **180**, 2582 (2009).
[50] M. Torrent, F. Jollet, F. Bottin, G. Zerah, and X. Gonze, Comput. Mater. Sci. **42**, 337 (2008).
[51] A. Lempicki and A. J. Wojtowicz, J. Lumin. **60**, 942 (1994).
[52] G. Bizarri and P. Dorenbos, Phys. Rev. B **75**, 184302 (2007).
[53] A. Baldereschi and N. O. Lipari, Phys. Rev. B **8**, 2697 (1973).
[54] M. Cococcioni and S. de Gironcoli, Phys. Rev. B **71**, 035105 (2005).

[55]R. Windiks, E. Winimer, L. Pourovskii, S. Biermann, and A. GeorgeS, J. Alloys Compd. **459**, 438 (2008).
[56]P. Dorenbos, E. van Loef, A. Vink, E. van der Kolk, C. van Eijk, K. Krämer, H. Güdel, W. Higgins, and K. Shah, J. Lumin. **117**, 147 (2006).
[57]J. L. F. Da Silva, Phys. Rev. B **76**, 193108 (2007).
[58]L. Pidol, B. Viana, A. Galtayries, and P. Dorenbos, Phys. Rev. B **72**, 125110 (2005).
[59]M. Joubert, S. Kazanskii, Y. Guyot, J. Gacon, J. Rivoire, and C. Pedrini, Opt. Mater. **24**, 137 (2003).
[60]M. Nikl, V. V. Laguta, and A. Vedda, Phys. Status Solidi B **245**, 1701 (2008).
[61]A. Bessiere, P. Dorenbos, C. van Eijk, K. Kramer, H. Gudel, C. Donega, and A. Meijerink, Nucl. Instrum. Methods Phys. Res. A **537**, 22 (2005).
[62]P. Dorenbos, J. Lumin. **108**, 301 (2004).
[63]E. van der Kolk, J. T. M. de Haas, A. J. J. Bos, C. W. E. van Eijk, and P. Dorenbos, J. Appl. Phys. **101**, 083703 (2007).
[64]W. Yen, M. Raukas, S. Basun, W. van Schaik, and U. Happek, J. Lumin. **69**, 287 (1996).
[65]C. Pedrini, Phys. Status Solidi A **202**, 185 (2005).
[66]W. Moses, S. Derenzo, M. Weber, A. Ray-Chaudhuri, and F. Cerrina, J. Lumin. **59**, 89 (1994).
[67]Comprehensive database of scintillation properties of inorganic materials [http://scintillator.lbl.gov/].
[68]H. Wiemhöfer, S. Harke, and U. Vohrer, Solid State Ion. **40-1**, 433 (1990).
[69]G. Bizarri and P. Dorenbos, J. Phys. Condens. Matter **21**, 235605 (2009).
[70]A. Srivastava, S. Camardello, H. Comanzo, M. Aycibin, and U. Happek, Opt. Mater. **32**, 936 (2010).
[71]S. A. Basun, T. Danger, A. A. Kaplyanskii, D. S. McClure, K. Petermann, and W. C. Wong, Phys. Rev. B **54**, 6141 (1996).
[72]C. Lushchik, E. Feldbach, A. Frorip, M. Kirm, A. Lushchik, A. Maaroos, and I. Martinson, J. Phys. Condens. Matter **6**, 11177 (1994).
[73]E. van Loef, P. Dorenbos, C. van Eijk, K. Kramer, and H. Gudel, J. Phys. Condens. Matter **14**, 8481 (2002).
[74]J. L. Yuan, X. J. Wang, D. B. Xiong, C. J. Duan, J. T. Zhao, Y. B. Fu, G. Bin Zhang, and C. S. Shi, J. Lumin. **126**, 130 (2007).
[75]J. Robertson, J. Vac. Sci. Technol. B **18**, 1785 (2000).
[76] S. Derenzo *et al.*, Nucl. Instr. and Meth. A (2010), doi: 10.1016/j.nima.2010.09.156.
[77]A. Chaudhry, A. Canning, R. Boutchko, Y. Porter-Chapman, E. Bourret-Courchesne, S. Derenzo, and N. Grønbech-Jensen, IEEE Trans. Nucl. Sci. **56**, 949 (2009).
[78]R. Boutchko, A. Canning, A. Chaudhry, R. Borade, E. Bourret-Courchesne, and S. Derenzo, IEEE Trans. Nucl. Sci. **56**, 977 (2009).
[79]P. Dorenbos, Chem. Mater. **17**, 6452 (2005).
[80]S. A. Chambers, T. Droubay, T. C. Kaspar, M. J. Gutowski, Vac. Sci.Technol., B **22**, 2204 (2004).
[81]S. S. Gatsono and E.V. Dulepov, Sov. Phys. Solid State **7**, 995 (1965).